In: Advances in Energy Research. Volume 23
Editor: Morena J. Acosta
ISBN: 978-1-63484-836-7

Chapter 5

INVESTIGATION OF THE ENERGY EFFICIENCY OF CONVENTIONAL AIR CONDITIONING SYSTEMS IN OFFICE BUILDINGS

Ioan Sarbu* and Marius Adam
Department of Buildings Services Engineering,
Polytechnic University Timisoara, Romania

ABSTRACT

Energy is vital for the progress and development of a nation's economy. In Europe, the ownership and electricity consumption of ventilation and air conditioning in buildings has been increasing for several decades. On the other hand, people's concerns about thermal comfort and indoor environment quality (IEQ) are increasing. The main purpose of most buildings and installed ventilating and air conditioning (VAC) systems is to provide an acceptable environment that does not impair the health and performance of the occupants.

Ventilation has long been known to have a major impact on a building's indoor air quality (IAQ) and comfort. Recent studies have demonstrated that air conditioning (AC) systems represent between 10 and 60% of the total energy consumption of office buildings.

Conventional AC systems, such as variable air volume (VAV), constant air volume (CAV) and fan-coil units (FCUs) air conditioning systems, supply cool air to spaces to remove thermal loads. A VAV system satisfies the health criterion and IAQ by supplying a minimum amount of fresh air based on national regulations and standards.

Conventional AC systems need a refrigeration plant (chiller) to produce cold water and a complex pipe network to distribute the cold water to the air conditioned spaces. Air-cooled chiller systems are commonly used in office buildings because of their flexibility. The coefficient of performance (COP) of the chiller directly influences the performance of the AC system. Compared to water-cooled chillers, air-cooled chillers are regarded as energy inefficient. This is due to the head pressure control (HPC) under

*E-mail: ioan.sarbu@upt.ro.

which the compression ratio of the condensing pressure to the evaporating pressure is kept high.

A possibility for improving the energy performance of a VAC system is the reduction of consumed electrical energy by adequate choices of the system configuration and control parameters. Among these parameters, the cooling mode of the cooled water chiller is very important. The VAC system must be complemented with an efficient control scheme to maintain comfort under any load conditions. Efficient control will also reduce energy use by keeping the process variables (temperature, pressure, etc.) at their set points.

One the main innovative contribution of this study consists in the achievement and implementation of an air-water mist cooled system for the air-cooled chillers of different VAC systems that has significant effect on the energy performance improvement of these systems. The experimental measurements are used to develop a mathematical model to minimise the power consumption by optimal control, depending only on non-controlled parameters (solar radiation intensity and outdoor air temperature) and to validate a TRNSYS (Transient Systems Simulation) simulation model for energy consumption of a VAC system.

This chapter provides a comparative study of the energy efficiency of a conventional VAC system with three configurations. This system was used to cool an experimental room in an office building in more control scenarios realised by adopting different cooled water temperatures and chiller cooling systems. In this purpose, an air-water mist cooled system for an air-cooled chiller is proposed. Depending on the components, the analysed VAC system has the following configurations: (1) air handling unit (AHU) and fan-coil units (FCUs); (2) air handling unit (AHU); and (3) heat recovery unit (HRU) and fan-coil units (FCUs). The electricity consumption weight of the equipment of each VAC system, the total energy consumption and the influence of control parameters on this consumption are analysed. The results of the experiments indicate that the optimal efficiency VAC system in office buildings includes an AHU and FCUs with an air-water mist cooled chiller and a cooled water temperature of 8°C. For this system, a mathematical model is developed to minimise the electricity consumption by optimal control, where the consumption depends only on non-controlled parameters (solar radiation intensity and outdoor air temperature). This model is verified with actual measurements to confirm its accuracy, and a good agreement between the prediction and measurement is achieved. Additionally, the assessment of thermal comfort in the experimental office is performed based on the PMV (predicted mean vote)-PPD (predicted percent dissatisfied) model using the ASHRAE Thermal Comfort program. The obtained results demonstrate that the AHU and FCUs system assures an increase in thermal comfort. A TRNSYS simulation model of energy consumption and PMV-PPD indices for the AHU and FCUs system is also developed and experimentally validated. Finally, this chapter analyses the indoor design air parameters with a simulation study from both views of thermal comfort and energy consumption.

1. INTRODUCTION

Energy is vital for the progress and development of a nation's economy. In Europe, the ownership and electricity consumption of ventilation and air conditioning in buildings has been increasing for several decades. On the other hand, people's concerns about thermal comfort and indoor environment quality (IEQ) are increasing. The main purpose of most buildings and installed ventilating and air conditioning (VAC) systems is to provide an acceptable environment that does not impair the health and performance of the occupants.

Ventilation has long been known to have a major impact on a building's indoor air quality (IAQ) and comfort [1]. Ventilation also has a very significant influence on the energy use in buildings, which represents approximately 40% of the total primary energy use in developed countries [2]. It is estimated that in those countries the energy use for ventilating and cooling residential and tertiary buildings often represents more than half of the total primary energy use and that air exchange with the outdoor environment, either by air infiltration or by proper ventilation, is one of the main aspects driving that use [3-5]. The relationship between ventilation of buildings and their energy use, however, is no simple matter, as it is dependent on a large number of variables. The influence of many of these variables has been explored individually in previous studies, such as air-flow control [6-8], heat recovery [9, 10], building air tightness [11] and humidity control [12].

Recent studies have demonstrated that air conditioning (AC) systems represent between 10 and 60% of the total energy consumption of office buildings [2]. An ongoing effort to simultaneously reduce the level of energy consumption and increase the leak-proofing of buildings is strictly connected to an increasing demand for cooling during the summertime. The higher demand for cooling is caused by the need to deliver fresh air to reduce the carbon dioxide (CO_2) concentration and to lower the temperature and humidity to permissible levels inside buildings as determined by the quality norms for the interior environment [13, 14].

Conventional AC systems, such as variable air volume (VAV), constant air volume (CAV) and fan-coil units (FCUs) air conditioning systems, supply cool air to spaces to remove thermal loads. A VAV system satisfies the health criterion and IAQ by supplying a minimum amount of fresh air based on national regulations and standards. The theory for the optimal supply air temperature in a VAV system is presented in [15]. There are three categories of AC systems that are used for comfort cooling: moveable units, fixed room air conditioners, and central systems. All three types of systems are used in both residential and public buildings, albeit to different degrees. In Europe, central systems are overwhelmingly found on non-residential buildings while most moveable units are used in dwellings. Fixed room air conditioners are used in both market sectors.

Conventional AC systems need a refrigeration plant (chiller) to produce cold water and a complex pipe network to distribute the cold water to the air conditioned spaces. Air-cooled chiller systems are commonly used in office buildings because of their flexibility. The operation of chillers usually takes up the highest proportion of the total electricity consumption of buildings [16]. The coefficient of performance (COP) of the chiller directly influences the performance of the AC system. Compared to water-cooled chillers, air-cooled chillers are regarded as energy inefficient. This is due to the head pressure control (HPC) under which the compression ratio of the condensing pressure to the evaporating pressure is kept high. The temperature of the air-cooled chiller is directly dependent on the ambient air temperature. This is of particular concern in areas with very hot weather in the summer.

To increase the performance of an air-cooled chiller, one of the best solutions is to decrease the condensation temperature. Thus, variable condensing temperature control (CTC) has been proposed as an alternative to HPC to lower the condensing temperature in air-cooled chillers [16, 17]. To reduce the condensing temperature, one of the easiest ways is the application of a direct evaporative cooler in front of the condenser to cool down the outdoor air temperature before it passes over the condenser. This approach results in a decrease in the compressor power of air-cooled chillers and the COP of the system could improve by 0.034-0.067 for each degree Celsius of pre-cooling provided [18]. Zhang et al. [19] investigated an

evaporative cooler filled with corrugated holed aluminium foil and presented correlations to predict the performance, pressure drop and temperature outlet of the cooler. He reported that the application of evaporative pre-coolers improves the COP of air-cooled chillers by 14.7% under the climatic conditions of Tianjin. Yu and Chan [20] simulated an air-cooled chiller equipped with a direct evaporative cooler and showed up to a 14.4% reduction in power consumption and up to a 4.6% increase in the refrigeration effect. The application of a direct evaporative cooler by injecting water on the media pad installed in front of the condenser of a window air conditioner unit was reported [21], and the COP could be improved by approximately 50% in regions with very hot weather conditions (approximately 50°C).

Variable speed control is another approach to decreasing compressor power because the motor efficiency can be improved at lower speeds when the chiller compressor is operating under a partial load [22, 23]. When a variable speed control is applied to the condenser fans, each fan can be operated at a lower speed with a large reduction in power while the condensing temperature remains at its set point.

A possibility for improving the energy performance of a VAC system is the reduction of consumed electrical energy by adequate choices of the system configuration and control parameters. Among these parameters, the cooling mode of the cooled water chiller is very important. The VAC system must be complemented with an efficient control scheme to maintain comfort under any load conditions. Efficient control will also reduce energy use by keeping the process variables (temperature, pressure, etc.) at their set points.

One the main innovative contribution of this study consists in the achievement and implementation of an air-water mist cooled system for the air-cooled chillers of different VAC systems that has significant effect on the energy performance improvement of these systems. The experimental measurements are used to develop a mathematical model to minimise the power consumption by optimal control, depending only on non-controlled parameters (solar radiation intensity and outdoor air temperature) and to validate a TRNSYS (Transient System Simulation) simulation model for energy consumption of a VAC system.

This chapter provides a comparative study of the energy efficiency of a VAC system with three configurations used to cool an experimental room in an office building in control scenarios involving different cooled water temperatures and compression chiller cooling systems. For this application, an air-water mist cooled system for the air-cooled chiller is proposed. Depending on the components, the analysed VAC systems have the following configurations: (1) air handling unit (AHU) and fan-coil units (FCUs); (2) air handling unit (AHU); and (3) heat recovery unit (HRU) and fan-coil units (FCUs). During the experimental program, the set point indoor air temperature was 25°C, according to Standard EN 15251 [24], and the outdoor air temperature, solar radiation intensity, cooling thermal energy and electrical energy consumed by the equipment of each VAC system were measured. The electricity consumption weight on the equipment of each VAC system, the total energy consumption and the influence of control parameters on this consumption were analysed. The results of the experiments showed that the most efficient VAC system for office buildings consists of an AHU and FCUs with an air-water mist cooled chiller and a cooled water temperature of 8°C. For this system, a mathematical model is developed to minimise the electricity consumption by optimal control, depending only on non-controlled parameters. This model is verified with actual measurements to confirm its accuracy and a good agreement between the prediction and measurement is achieved. Additionally, the assessment

of thermal comfort in the experimental office is performed based on the PMV (predicted mean vote)-PPD (predicted percent dissatisfied) model using the ASHRAE Thermal Comfort program. The obtained results demonstrated that the system with an AHU and FCUs assures an increase in thermal comfort. A simulation model in a TRNSYS program for energy consumption and PMV-PPD indices for the AHU and FCUs system is also developed and experimentally validated. Finally, this chapter analyses the indoor design air parameters with a simulation study from both views of thermal comfort and energy consumption.

2. DESCRIPTION OF THE EXPERIMENTAL OFFICE ROOM

The building under consideration is an eight story office building located in Timisoara, Romania. It contains a total air conditioned floor area of 8260 m^2. The city has a continental temperate climate with four different seasons and the demand for cooling is observed between 1 May and 30 September. The cooling load was calculated for four construction solutions:

A. Building with an upper glass quality surface (quality window coefficient $c_1 = 0.27$) with exterior shading elements (shielded window coefficient $c_2 = 0.2$);
B. Building with an upper glass quality surface ($c_1 = 0.27$) without exterior shading elements ($c_2 = 1.0$);
C. Building with a glass area made by a double leaf window with thick windows ($c_1 = 0.8$) and exterior shading elements ($c_2 = 0.2$);
D. Building with a glass surface ($c_1 = 0.8$) without exterior shading elements ($c_2 = 1.0$).

The following operating data in the building are known: 730 occupants, with a heat rejection of 130 W/person; 660 computers, with a heat rejection of 300 W/comp; and electric power for light sources of 10 W/m^2. The results are summarised in Table 1. It is found that the energy optimal solution for this office building is solution (A) with the lowest cooling load Q_{cool} = 438.7 kW. An experimental room is located in this building, which can be divided into different thermal zones (Figure 1) depending on the orientation of the exterior walls and the floor where the room is located.

The experimental room (Figure 2) has an area of 47 m^2 and its height is 3.70 m. The envelope is made of 200 mm porous brick with a 100 mm thermal insulating layer and 20 mm of lime mortar. The heat transfer resistances (1/*U*-values) are as follows: walls 2.90 m^2K/W and double-glazed windows 0.45 m^2K/W. The window area is 17 m^2 and the area of the interior door is 2.1 m^2. The indoor air design temperature is 25°C and the outdoor air design temperature is 32.6°C for the cooling season. The number of room occupants is two, each having one computer. The electric lighting has a heat yield of 5 W/m^2.

Table 1. Cooling load for office building

Solution	Q_{cool}
A	438.7
B	566.2
C	501.3
D	879.2

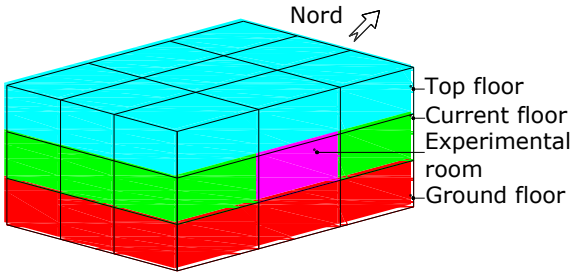

Figure 1. Thermal zoning of the office building.

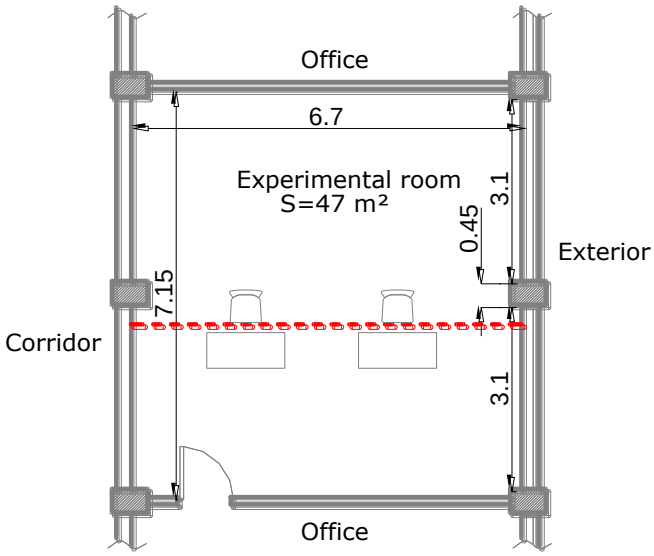

Figure 2. Experimental room.

The calculation was performed for the climate conditions of the city of Timisoara, resulting in a cooling load of Q_{cool} = 3.28 kW. The monthly cooling energy consumption is summarised in Table 2.

Table 2. Monthly cooling energy consumptions

Month	Cooling load [W]	Operating hours per day	Days	Consumed energy [kWh/month]
May	2923.70	6	31	543.81
June	3163.08	8	30	759.14
July	3270.00	12	31	1216.44
August	3197.89	11	31	1090.48
September	2950.13	6	30	531.02
Total				4140.89 kWh/season

3. DESCRIPTION OF THE EXPERIMENTAL VAC SYSTEM

The experimental VAC system is located in the office room and consists of the following equipment (Figure 3): an air-cooled Daikin chiller, a GEA air handling unit, a Stiebel Eltron plate heat recovery unit, and two wall fan-coil units [25].

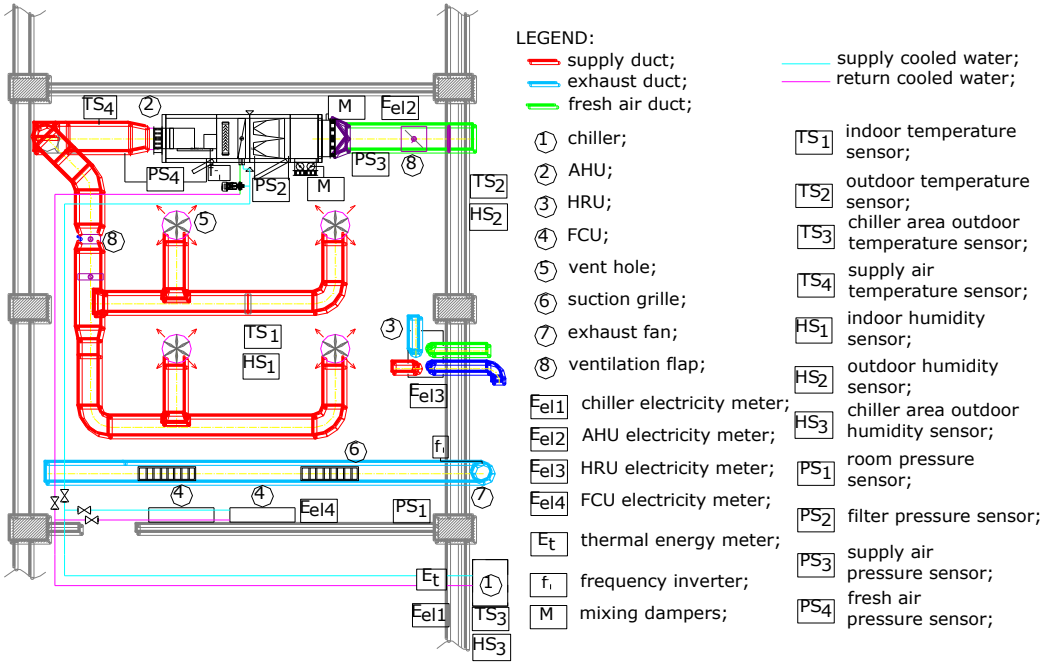

Figure 3. Schematic of the location of the equipment in the experimental room.

3.1. Chiller

The cool carrier fluid used in the investigated VAC systems is cooled water obtained with the air-cooled chiller having a swing compressor working with R410A refrigerant and a nominal cooling power (capacity) of 7.1 kW rated under the operating conditions of the entering condenser air temperature t_e = 35°C, entering chilled water temperature t_{cw} = 7°C and a water temperature drop in the evaporator Δt = 5°C. The chiller operates under HPC with a constant speed condenser fan. The cooling power Q_0 and the electrical power P_e values of the chiller for different t_e and t_{cw} temperatures are presented in Table 3.

The start-up of the chilleris performed using a Daikin remote control, type ARC448A2, that controls the compressor depending on the outlet cooled water temperature. The set point of the cooled water temperature can be between 5 and 22°C.

The air-cooled system of the chiller condenser can be modified by using an evaporative cooled air condenser to decrease the outdoor air temperature in the chiller area up to the wet bulb temperature based on an isenthalpic process. To decrease the temperature of the ambient air, the entering condenser air is precooled with a water mist circuit coupled to the air-cooled condenser. Thus, a water spraying system with four nozzles is mounted in front of the air-

cooled condenser to produce the water mist (Figure 4). The water mist circuit was equipped with a pressure pump at a rating of 0.55 kW and the water was forced through nozzles to create a mist of under 50 μm droplets. The water circulation flow rate was constant for all tests. The outdoor air temperature t_e and the relative humidity RH_e were measured before and after the water spraying process to determine the optimal mounting distance between the nozzles and the air-cooled condenser surface. The recorded values before the water spraying were t_e = 28°C and RH_e = 60% and the recorded values after the water spraying are presented in Table 4. The nozzles were mounted at a distance of 0.2 m from the condenser surface because the lowest outdoor air temperature of 22.2°C and a relative humidity of 98% were identified at this distance.

Table 3.Variation of cooling power Q_0 and electrical power P_e for chiller

t_{wr} [°C]	t_e [°C]							
	20		25		30		35	
	Q_0 [kW]	P_e [kW]	Q_0 [kW]	P_e [kW]	Q_0 [kW]	P_e [kW]	Q_0 [kW]	P_e [kW]
7	8.31	2.23	7.94	2.46	7.54	2.70	7.10	2.95
11	9.31	2.31	8.89	2.55	8.44	2.81	7.49	2.94
13	9.82	2.35	9.39	2.60	8.91	2.86	7.78	2.91
16	10.6	2.41	10.15	2.67	9.65	2.94	8.23	2.85
20	11.7	2.49	11.20	2.76	10.67	3.05	8.82	2.76

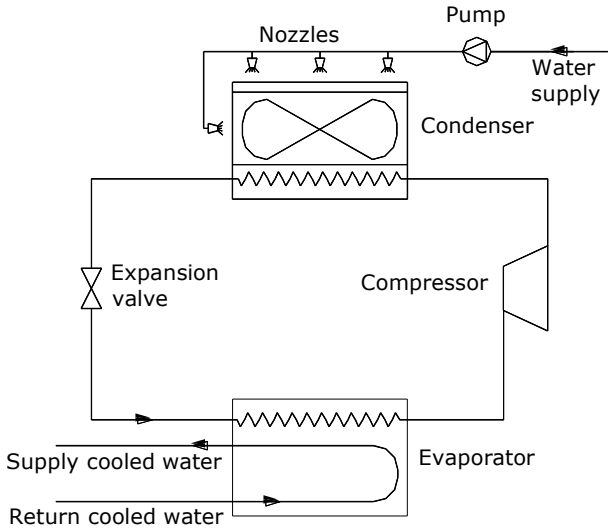

Figure 4. Schematic of the chiller and water mist system.

The operation of a chiller is characterised by the coefficient of performance(COP), which is defined as the ratio between the useful effect produced (useful cooling energy E_{cool}, in kWh) and the energy consumed to obtain it (electrical energy E_{el}, in kWh):

$$\mathrm{COP} = \frac{E_{cool}}{E_{el}} \tag{1}$$

If both the usable energy (E_{cool}) and the consumed energy (E_{el}) are summed during a season (year), the seasonal coefficient of performance ($\mathrm{COP}_{seasonal}$) is obtained by Eq. (1).

Table 4. Mounting distance of nozzles

Mounting distance [m]	Outdoor air temperature after spraying, t_e [°C]	Outdoor air relative humidity after spraying, RH_e[%]
0.40	24.2	83
0.35	23.6	87
0.30	23.1	91
0.20	22.2	98

The energy efficiency of the chiller operating at full load in cooling mode is expressed by the EER (Energy Efficiency Ratio). The EER, in Btu/(Wh), is defined by the equation:

$$\mathrm{EER} = \frac{Q_0}{P_e} \tag{2}$$

where Q_0 is the cooling power of the chiller in British thermal units per hour (Btu/h) and $P_e$is the drive power of the chiller in W.

The coefficient of performance of the chiller in cooling mode is obtained by the equation:

$$\mathrm{COP} = \frac{\mathrm{EER}}{3.412} \tag{3}$$

where 3.412 is the transformation factor from Watts to Btu/h.

In Europe, the evaluation index of cooling energy efficiency for chiller operation at a partial load ratio, the European Seasonal Energy Efficiency Ratio (ESEER), is defined by the equation:

$$\mathrm{ESEER} = \frac{1 \cdot \mathrm{EER}_{100\%} + 42 \cdot \mathrm{EER}_{75\%} + 45 \cdot \mathrm{EER}_{50\%} + 12 \cdot \mathrm{EER}_{25\%}}{100} \tag{4}$$

where $\mathrm{EER}_{100\%}$, $\mathrm{EER}_{75\%}$, $\mathrm{EER}_{50\%}$ and $\mathrm{EER}_{25\%}$ are the respective energy efficiencies of the chiller operating at different partial load ratios (100%, 75%, 50% and 25%) calculated for the outdoor air temperatures recommended in [26].

The EER values of a chiller operating at full load are calculated by applying Eq. (2) and (3) and the ESEER values depending on chiller efficiencies at partial load ratios and are determined for both chiller cooled modes. The results of the calculations for the two condenser types, different outdoor air temperatures (t_e), and cooled water temperatures (t_{cw}) at 5 and 8°C are summarised in Table 5. It is found that the ESEER values obtained for the air-water mist cooled chiller, 12.15% and 13.21%, are higher than the ESEER values obtained for

the air cooled chiller, 13% and 13.7%. A comparison of the results of the two chiller cooling modes shows that as the ambient temperature increases, the effect of using evaporative air pre-cooling also increases. Under HPC with water mist pre-cooling, the chiller EER increased by up to 24.8-30.8%. These results are consistent with other findings in the literature [19]. Decreasing the EER of the evaporative cooled air condenser with outdoor air temperature is the result of increasing the air temperature in the condenser area. The energy savings produced by water mist pre-cooling are expected to be more significant when the chiller operates in a hot and arid climate.

Table 5. Energy efficiency of chiller

t_{cw} [°C]	Chiller cooling mode	t_e [°C]				ESEER [–]	Percentage difference [%]
		20	25	30	35		
		EER [–]					
5	Air	12.72	11.02	9.53	8.21	10.57	13.0
	Air-water mist	14.11	12.55	11.21	10.92	12.15	
8	Air	13.76	11.90	10.25	8.70	11.40	13.7
	Air-water mist	15.35	13.67	12.14	11.78	13.21	

3.2. Air Handling Unit

The AHU has a maximum air flow rate of 2700 m^3/h and consists of a mixing chamber, a sensitive filter of class F5, a cooling coil, and a supply centrifugal fan with variable speed and a maximum pressure loss of 250 Pa. A pressure sensor located on the fresh air duct provides the minimum fresh air flow rate (Figure 5).

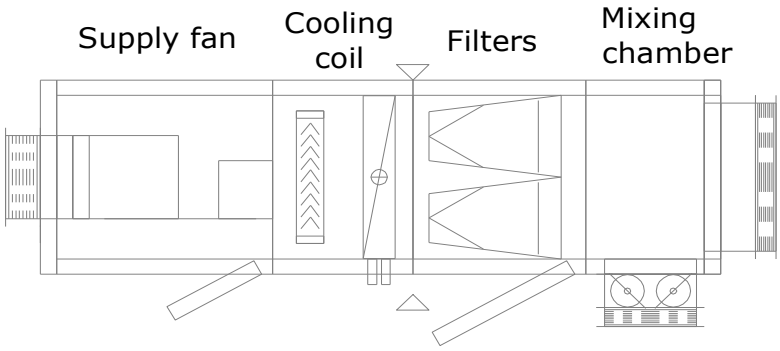

Figure 5. Schematic of the air handling unit.

3.3. Heat Recovery Unit

The heat recovery unit (HRU) has an air flow rate of 354 m^3/h and uses two fans and four separate ducts for the supply and exhaust air. The fresh air goes through the filter of the HRU and is supplied to the room. Return air goes through the cross-countercurrent HRU and is exhausted outside. In this way, the energy from the exhaust air is transferred to the fresh air. An efficient cross-countercurrent heat exchanger can recover up to 90% of the latent energy in the extracted air.

A low noise level is achieved by slowly rotating the fans. HRU fans can operate at three speed steps. For each speed step, there is a corresponding air flow rate: when the room is occupied, when the room is not occupied and when there are more people in the room and the CO_2 concentration is high.

The temperature efficiency of the HRU, η_{HRU} in %, is defined by the equation:

$$\eta_{HRU} = \frac{t_1'' - t_1'}{t_2' - t_1'} 100 \tag{5}$$

where t_1', t_1'' are the initial and final temperatures of the fresh air and t_2' is the initial temperature of the exhaust air.

3.4. Fan-Coil Units

The terminal equipment is the cooling coil (CC) from an AHU and two FCUs, one a Climaventa type and the other a Rhoss type, with a total cooling power of 3.2 kW.

3.5. VAC System Configurations

Depending on the component equipment (Figure 3), three different configurations of VAC system are studied and compared:

(1) Air handling unit (AHU) and fan-coil units (FCUs). The air exchange rate of $n = 2\ h^{-1}$ is achieved with an AHU at a temperature equal to the set point indoor air temperature t_i and the space is cooled with the FCUs. The air is conditioned by the cooling coil, which is located inside the AHU. Air is supplied to the conditioned space via ducting and is returned from the space via grills and ducts located outside the building. Fresh air is supplied to the experimental room by diffusers. The AHU works with 100% fresh air. The water cooled chiller supplies chilled water to all of the cooling coils, including those of the FCUs. Indoor temperature control is achieved with the FCUs.

(2) Air handling unit (AHU). The ventilation and air conditioning of the space is achieved by an AHU with a variable air flow rate (depending on the cooling load) at a temperature of 18°C. The operation of mixing dampers takes into consideration the minimum fresh air percentage and the use of fresh air for cooling when possible,

thereby improving efficiency. If the indoor (return) temperature is less than the fresh air temperature, then the mixed air flow rate includes the minimum fresh air ratio. If the fresh air temperature is between the supply temperature and the indoor temperature, the dampers will deliver 100% fresh air and the mix temperature will be equal to the fresh air temperature.

(3) Heat recovery unit (HRU) and fan-coil units (FCUs). The air exchange rate of $n = 2$ h^{-1} is achieved with an HRU and the space is cooled with FCUs. During the warmer seasons, the system precools and dehumidifies the supplied fresh air. The water-cooled chiller supplies chilled water to the cooling coils of the FCUs, which control the indoor temperature. The use of proper ventilation recovery is the most cost efficient, sustainable and quickest way to reduce total energy consumption, give better IAQ and protect the building.

Regardless of the used configuration, an in-room mast ensures the thermal comfort parameters are satisfied ($24.5°C \leq t_i \leq 25.5°C$, RH_i = 40-60%) [24].

The indoor, outdoor, chiller area and supply air temperatures are measured by temperature sensors TS_1, TS_2, TS_3 and TS_4, respectively. The indoor, outdoor and chiller area air humidity levels are measured by humidity sensors HS_1, HS_2 and HS_3, respectively. The room, filter, supply and fresh air pressures are measured by pressure sensors PS_1, PS_2, PS_3 and PS_4, respectively. These sensors are connected to a programmable logic controller (PLC).

The COP of the VAC system (COP_{syst}) is defined by Eq. (1), where E_{el} is the electrical energy consumption of the VAC system, which includes the energy consumption of all equipment (chiller, pressure pump of the water mist circuit, fans of the FCUs, the fan of the HRU, the supply fan of the AHU, exhaust fan, frequency converters, and the PLC) in the system configuration.

The total consumed energy will depend on the component efficiencies, such as the specific fan power value, the temperature efficiency of the heat recovery unit and the chiller coefficient of performance.

4. MEASURING APPARATUS

A network of sensors was set up to monitor the most relevant parameters of the system [25]. NTC (Negative Temperature Coefficient) temperature sensors were used to measure the indoor, outdoor and supply air temperatures. The temperature sensors were four PT500 wires with an accuracy of ±0.15°C. Three humidity sensors with output signal voltage (0-10 V) are used to measure the indoor and outdoor air humidity with an accuracy of ±2.5%.

One thermal energy meter was used to measure the cooling energy produced by the compression chiller. The thermal energy meter was built with a heat computer, two PT500 temperature sensors and an ultrasonic mass flow meter. The thermal energy meter was a KAMSTRUP meter, model Multikal 402, with an IP 67 signal converter and an accuracy of <0.2%. A three phase electronic electricity meter measured the electrical energy consumed by the AHU (the supply fan, the exhaust fan and two frequency converters). The electronic electricity meter was a multifunctional electricity meter from AEM (model CST 0410), with an accuracy grade of ±0.4% of the nominal value. Three monophase electronic electricity

meters from AEM (model CSM 0201) measured the electrical energy consumed by the chiller (including the water mist circuit pump and the PLC), the HRU, and the FCUs, respectively, with an accuracy grade of ±0.5% of the nominal values.

The monitoring and recording of the experiments were performed using a data acquisition system PLC (SIEMENS model Simantic S7-300) and a PC computer running the Windows operating system that was used to run the IntelliMONITOR program for capturing and processing the data.

The ground-reflected radiation is measured with an LP PYRA05 albedometer, which consists of two first class pyranometers mounted in opposition. One of the pyranometers measures the global solar radiation, while the other measures the reflected solar radiation. The main meteorological parameters, temperature, air pressure and relative humidity, are also recorded in standard conditions with the Delta OHM HD2001.1 pyranometer located in the Solar Radiation Monitoring Station (SRMS) of Timisoara [27]. The sensors are integrated into an acquisition data system based on a National Instruments PXI Platform consisting of a PXI-8105 controller with a Core Duo 2 GHz processor running Windows XP and a PXI-6259 data acquisition board optimised for high accuracy.

5. EXPERIMENTAL RESULTS

The VAC system was monitored for two months. The experiments were conducted from the 3 July 2013 to 28 August 2013 [25].

5.1. Monitoring and Analysis of Electricity Consumption of System Equipment

To determine the energy performance of the three configurations of the VAC system described above, four control scenarios were performed by modifying the temperature of the cooled water at the evaporator outlet and the chiller cooling mode, as shown in Table 6. The indoor air temperature was set to the comfort value of 25 ° C and the measurements were taken for 8 hours per day at 30 minute intervals for each scenario. In all scenarios, the cooling energy, the electrical energy consumed by each of the analysed systems, the indoor and outdoor air temperatures and the global solar radiation intensity were measured.

Table 6. Scenarios for system operating control

Scenario	Chiller cooling mode	Water cooled temperature t_{wr} [°C]
1	Air	5
2	Air-water mist	5
3	Air	8
4	Air-water mist	8

The electricity consumption values E_{el} measured for each VAC system and control scenario are summarised in Table 7. Analysis of the results of the four scenarios shows that the best energy efficiency is achieved in scenario 4 for all three VAC systems, where the electricity consumption is 14.97 kWh, 18.94 kWh, and 4.72 kWh, respectively. Henceforth, this is the scenario used in the remainder of the analysis.

Table 7. Electricity consumption E_{el}, in kWh

Scenario	Equipment	VAC System		
		AHU and FCUs	AHU	HRU and FCUs
1	Chiller	8.36	10.17	7.15
	AHU	8.67	19.37	–
	FCUs	0.37	–	0.52
	HRU	–	–	0.54
	Total	17.40	29.54	8.21
2	Chiller	5.98	6.81	4.24
	AHU	8.67	14.17	–
	FCUs	0.62	–	0.46
	HRU	–	–	0.58
	Total	15.27	20.98	5.28
3	Chiller	7.87	9.03	6.64
	AHU	8.67	18.21	–
	FCUs	0.66	–	0.62
	HRU	–	–	0.58
	Total	17.20	27.24	7.84
4	Chiller	5.59	6.23	3.66
	AHU	8.67	12.71	–
	FCUs	0.71	–	0.51
	HRU	–	–	0.55
	Total	14.97	18.94	4.72

5.1.1. Electricity Consumption Weight of the AHU and FCUs System Equipment

The components of the AHU and FCUs system are the chiller, the AHU and the FCUs. Figure 6 illustrates that the weight of electricity consumed by the chiller is only 37.3% (5.59 kWh) due to higher power consumption by the AHU, which registered 57.9% (8.67 kWh). The AHU consumes more power than chiller because the AHU is equipped with a three phase fan motor driver and the chiller is equipped with components (compressor, fan, pump) having monophase motors. The electrical consumption of the FCUs is below 5% of the total consumption of electricity in the system (14.97 kWh). To reduce the electricity consumption of the system, the energy efficiency of the chiller must be improved while the specific fan power of the AHU must be reduced.

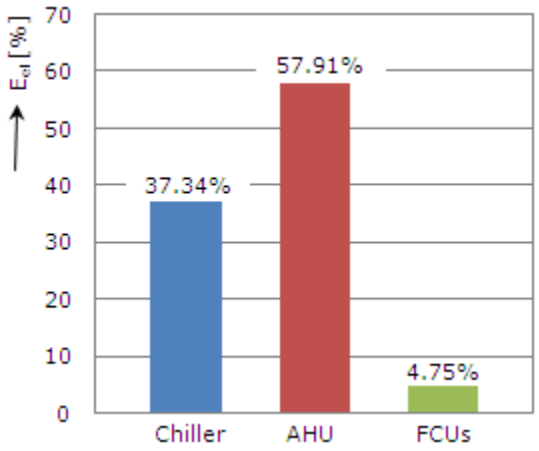

Figure 6. Electricity consumption weight for the AHU and FCUs system equipment.

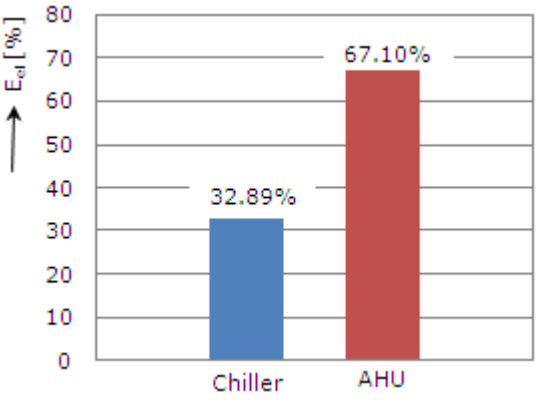

Figure 7. Electricity consumption weight for the AHU system equipment.

5.1.2. Electricity Consumption Weight of the AHU System Equipment

The components of the AHU system are the chiller and an AHU that provides a variable air flow rate at a temperature of 18°C to achieve the indoor air temperature set point of 25°C. The chiller electrical consumption weight decreases to approximately 33.0% of the total electricity consumption of the system (Figure 7) even if the absolute power consumption of the chiller increases to 6.23 kWh (Table 7). The absolute power consumption of the AHU increases to 18.94 kWh because the air flow rate is higher. This means that a reduction in the energy consumption of the entire system requires a decrease in the specific fan power of the AHU.

5.1.3. Electricity Consumption Weight of the HRU and FCUs System Equipment

In the HRU and FCUs system, the AHU is replaced by a heat recovery unit that provides a fresh air flow rate and energy consumption that is distributed differently than in the AHU and FCUs system so the electrical consumption of the FCUs increases to 10.8% (Figure 8). Additionally, Figure 8 shows that the chiller has the largest weight of electricity consumption at 77.5%, followed by the HRU (11.7%).

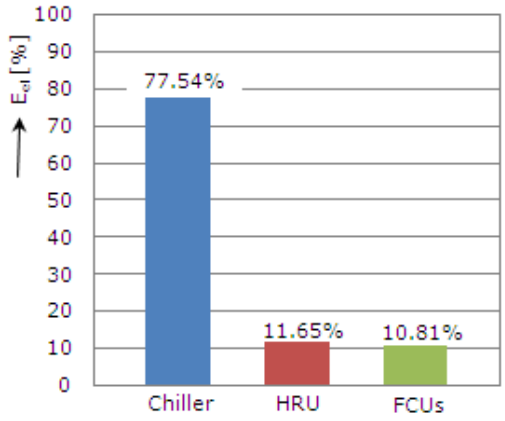

Figure 8. Electricity consumption weight for the HRU and FCUs system equipment.

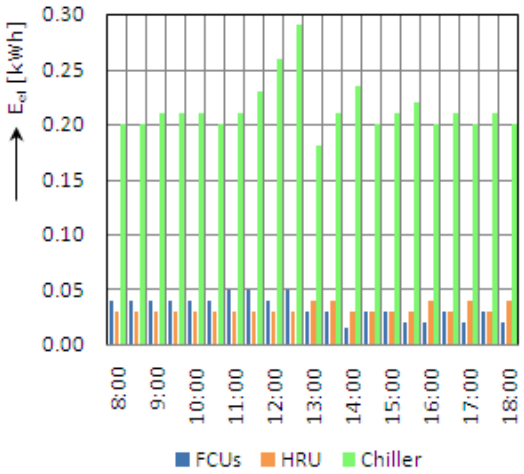

Figure 9. Variation of the hourly electricity consumption of equipment.

The hourly variation of energy consumption of the equipment illustrated in Figure 9 indicates that the electricity consumption of the FCUs has a higher value (0.05 kWh) of the total power consumption of 0.36 kWh until 12:30, when due to increased solar radiation intensity and large glass surfaces, the experimental room cooling load is the highest. After 12:30, the electrical consumption of the FCUs decreases until it is 0.015 kWh that is only 5.5% of the total energy consumption of 0.28 kWh.

5.2. Influence of Control Parameters on the Electricity Consumption

The influence of control parameters (chilled water temperature, chiller cooling mode) on the total electricity consumption was investigated by comparing two operating scenarios at a time for each VAC system.

5.2.1. Cooled Water Temperature

To determine the influence of chilled water temperature on the electricity consumption, scenario 1 is compared to scenario 3 and scenario 2 is compared to scenario 4 for each VAC system.

The electricity consumption E_{el} and the COP_{syst} of the three VAC systems for the scenarios are presented in Table 8, which shows the energy savings ΔE_{el}. It is found that for the three systems (AHU and FCUs, AHU and HRU and FCUs), an electrical energy saving ΔE_{el} was achieved when the cooled water temperature increased from 5°C (scenarios 1 and 2) to 8°C (scenarios 3 and 4).

Table 8. Influence of cooled water temperature on electricity consumption

VAC System		Scenario			
		1	3	2	4
AHU and FCUs	E_{el} [kWh]	17.40	17.20	15.27	14.97
	ΔE_{el} [%]	1.15		1.96	
	COP_{syst}	1.93	1.95	2.20	2.24
	COP variation [%]	2.0		1.8	
AHU	E_{el} [kWh]	29.54	27.24	20.98	18.94
	ΔE_{el} [%]	7.78		9.72	
	COP_{syst}	1.14	1.23	1.60	1.77
	COP variation [%]	7.3		9.6	
HRU and FCUs	E_{el} [kWh]	8.21	7.84	5.28	4.72
	ΔE_{el} [%]	4.50		10.60	
	COP_{syst}	4.09	4.29	6.36	7.12
	COP variation [%]	4.7		10.7	

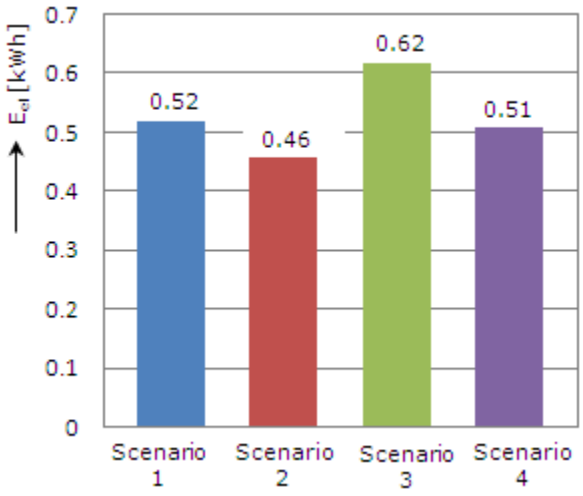

Figure 10. Electricity consumption of the FCUs from the HRU and FCUs system.

A comparison of the data in Table 8 shows that of all the solutions analysed, the HRU and FCUs system with an air-water mist cooled chiller and a cooled water temperature of 8°C

(scenario 4) has the minimum energy consumption of 4.72 kWh, a maximum energy saving of 10.60% and a maximum COP_{syst} of 7.12. Although this approach resulted in an energy savings of 1.96% for the AHU and FCUs system, which is less than the AHU system energy savings of 9.72%, the AHU and FCUs system has a COP_{syst} = 2.24 that is superior to the COP_{syst} = 1.77 of the AHU system because the electricity consumption is lower in the first case. Additionally, the influence of the evaporative cooled chiller on the COP_{syst} improvement from 4.7 to 10.7 is more significant for the HRU and FCUs system than it is for the AHU and AHU and FCUs systems because the weight of the chiller electricity consumption is 77.54% (Figure 8) compared to approximately 35% for the other two systems (Figures 6, 7). An analysis of the electricity consumption in the HRU and FCUs system (air conditioning part) shows that the minimum energy consumption of 0.46 kWh per terminal unit (Figure 10) is obtained when the chiller is cooled with air-water mist and the cooled water temperature is 5°C (scenario 2).

5.2.2. Chiller Cooling Mode

To study the influence of the chiller cooling mode on electricity consumption, scenario 1 is compared to scenario 2 and scenario 3 is compared to scenario 4 for each VAC system. Table 9 presents a comparison of the electricity consumption E_{el} and the COP_{syst} of the three VAC systems in the two by two scenarios, resulting in the energy savings ΔE_{el}. It is found that for all three systems (AHU and FCUs, AHU and HRU and FCUs) an energy saving ΔE_{el} is detected when using an air-cooled chiller with a water mist system (scenarios 2 and 4).

Table 9. Influence of chiller cooling mode on electricity consumption

VAC system		Scenario			
		1	2	3	4
AHU and FCUs	E_{el} [kWh]	17.40	15.27	17.20	14.97
	ΔE_{el} [%]	12.24		12.96	
	COP_{syst}	1.93	2.20	1.95	2.24
	COP variation [%]	12.3		12.9	
AHU	E_{el} [kWh]	29.54	20.98	27.24	18.94
	ΔE_{el} [%]	28.98		30.47	
	COP_{syst}	1.14	1.60	1.23	1.77
	COP variation [%]	28.8		30.5	
HRU and FCUs	E_{el} [kWh]	8.21	5.28	7.84	4.72
	ΔE_{el} [%]	35.84		39.79	
	COP_{syst}	4.09	6.36	4.29	7.12
	COP variation [%]	35.7		39.7	

The data in Table 9 show that of all the solutions analysed, the HRU and FCUs system with an air-water mist cooled chiller and a cooled water temperature of 8°C (scenario 4) has the minimum energy consumption of 4.72 kWh, the maximum energy saving of 39.79% and the maximum COP_{syst} of 7.12. While this approach results in an energy savings of only 12.96% for the AHU and FCUs system, which is lower than the 30.47% energy savings of the AHU system, the AHU and FCUs system has a COP_{syst} = 2.24 that is superior to the COP_{syst} = 1.77 of the AHU system because the energy consumption is lower in the first case. The

application of evaporative chiller cooling improves the COP_{syst} with 12.24%, 28.8% and 35.7% for the AHU and FCUs, AHU and HRU and FCUs systems, respectively at a cooled water temperature of 5°C and 12.9%, 30.5% and 39.7%, respectively, for a cooled water temperature of 8°C.

Although the experimental results (Tables 8 and 9) show that the HRU and FCUs system has the largest COP_{syst} of 7.12, this system is not recommended for office buildings because the architecture of the building would be affected by the application of various ventilation grills on the facade. Therefore, the AHU and FCUs system using the air-water mist cooled chiller and a cooled water temperature of 8°C with a $COP_{syst} = 2.24$ is recommended.

5.3. Uncertainty Analysis

Error analysis for estimating the maximum uncertainty in the experimental results was performed [28]. It was found that the maximum uncertainty in the results is in the COP_{syst}, with an acceptable uncertainty range of 4.8-8.9%. The root sum square error of the chiller EER due to the uncertainties of the individual variables was evaluated to be 0.34 for an EER value of 8.7 at the design condition. The uncertainty of the EER was 3.9%.

6. Optimal Control of Energy Consumption

Global optimisation methods of cooling systems using electronic controllers have been studied by Sud [29] and Lau [30]. Braun [31] developed a methodology for determining the optimal control strategy of a VAC system using quadratic variables of continuous controlled and uncontrolled variables to express the energy consumed by a cooling system. Ulleberg [32] designed a controller for a Building Management System (BMS). By analysing the behaviour of the VAC system in real time, the controller allows energy consumption optimisation by using an optimal control based on the supply air temperature and the cooled water temperature.

In this chapter, a mathematical model of the electricity consumption of a VAC system that depends on two controlled variables (cooled water temperature and indoor air temperature) and two uncontrolled variables (solar radiation intensity I and outside air temperaturet_e) as parameters is developed. The calculated values of the controlled variables that minimise the energy consumption of the cooling system depend on the uncontrolled variables. The values of the uncontrolled variables are measured by a real-time controller, yielding the optimal values of the controlled variables.

6.1. Mathematical Model of the Electricity Consumption Function

The electrical consumption depends on the controlled variables u, the uncontrolled variables f and the discrete variables M. The discrete variables M are those adjustments that have discrete settings, such as the high and low speed of the fan and the number of chillers, fans and pumps in operation.

By denoting an *F*-energy function, the mathematical model has the following general expression:

$$F = F(u, f, M) \tag{6}$$

The model used in this analysis has the following form:

$$F = F(u_1, u_2, f_1, f_2) \tag{7}$$

where the cooled water temperature (u_1) and the indoor air temperature (u_2) can vary continuously in the adjustment range and f_1 and f_2 are the solar radiation intensity and the outdoor air temperature. In addition, each of these variables can have limits. These constraints must be considered in the optimisation process.

Braun [31] showed that the energy consumption of chillers, fans and pumps can be adequately expressed by quadratic functions. Therefore, the energy consumption function (7) has the general form:

$$F = \mathrm{uAu}^T + \mathrm{fCf}^T + \mathrm{fEu}^T + \mathrm{bu}^T + \mathrm{df}^T + g \tag{8}$$

where A, C and E are symmetric matrices, b and d are coefficient vectors and g is a scalar. Similarly, in the studied case, it can be written:

$$\begin{aligned} F = {} & (u_1, u_2)\begin{bmatrix} a_{11} & a_{12} \\ a_{12} & a_{22} \end{bmatrix}\begin{bmatrix} u_1 \\ u_2 \end{bmatrix} + (f_1, f_2)\begin{bmatrix} c_{11} & c_{12} \\ c_{12} & c_{22} \end{bmatrix}\begin{bmatrix} f_1 \\ f_2 \end{bmatrix} + \\ & (f_1, f_2)\begin{bmatrix} e_{11} & e_{12} \\ e_{12} & e_{22} \end{bmatrix}\begin{bmatrix} u_1 \\ u_2 \end{bmatrix} + (b_1, b_2)\begin{bmatrix} u_1 \\ u_2 \end{bmatrix} + (d_1, d_2)\begin{bmatrix} f_1 \\ f_2 \end{bmatrix} + g \end{aligned} \tag{9}$$

All coefficients of Eq. (9) are determined by linear regression using data from the measurements. The total number of possible coefficients in the quadratic function (9) is [31]:

$$N_c = N_u^2 - \frac{N_u(N_u - 1)}{2} + N_u + N_f^2 - \frac{N_f(N_f - 1)}{2} + N_f N_u + N_f + 1 \tag{10}$$

where N_u is the number of controlled variables and the N_f is the number of uncontrolled variables.

In this study, $N_u = 2$ (cooled water temperature u_1 and air indoor temperature u_2) and $N_f = 2$ (solar radiation intensity f_1 and outdoor air temperature f_2), so that Eq. (10) results in $N_c = 15$ unknown coefficients.

Using specialised software (Mathematica 6.0) and the measured data, the expression of function *F* is obtained by quadratic linear regression. To obtain the minimum of the function *F*, Fermat's theorem (partial derivatives calculated in local extreme points are equal to zero) is applied and the Hessian matrix is conditioned to be positive definite.

For the function given by Eq. (8), by considering *u* as a variable and *f* as a parameter, the relationship is obtained:

$$u = -\frac{1}{2}\mathbf{A}^{-1}\mathbf{b} - \frac{1}{2}\mathbf{A}^{-1}\mathbf{E}\mathbf{f} \tag{11}$$

Eq. (11) provides values of the controlled variables that optimise F where the matrix $\mathbf{A}$ is positive definite.

6.2. Application for AHU and FCUs System

The AHU and FCUs air conditioning system cools the office rooms by controlling the AHU supply fan speed, the FCUs fans speed, the cooled water temperature and the supply air temperature. The system has two controlled variables: the cooled water temperature t_{cw} and the indoor air temperature t_i. The important uncontrolled variables are the solar radiation intensity I and the outdoor air temperature t_e. By analysing the energy consumption for different values of solar radiation intensity (u_1) and outdoor temperature (u_2), it is observed that the uncontrolled variable u_1 has a greater influence on the consumption of electricity.

Initially, the variables' values for optimum control are unknown. Therefore, a wide range of controlled variables (t_i, t_{cw}) and uncontrolled variables (I, t_e) have been used as parameters in the simulation. Uncontrolled variables included the full range of possible conditions. In the next step, the controlled variables have been adjusted to be close to the expected optimal conditions. These steps were repeated until the optimum controlled variable values were found.

The values of the two controlled variables are limited to avoid issues with the operation of the system components. Cooled water temperature is limited between 5ºC and 8ºC to provide sufficient dehumidification and to prevent freezing in the evaporator tubes. Indoor air temperature is limited between 24ºC and 25.5°C to avoid subcooling or overheating of the air conditioned spaces.

Considering such a set of measurements with a cooled water temperature of 5°C and using linear regression, the electricity consumption function is obtained:

$$\begin{aligned} F(u_1, u_2, f_1, f_2) = {} & 30.4298 + 0.0483206 f_1 + 0.000211353 f_1^2 + \\ & 0.303137 f_2 + 0.00605557 f_1 f_2 + 0.0484248 f_2^2 + 6.08597 u_1 + \\ & 0.00966411 f_1 u_1 + 0.0606274 f_2 u_1 + 1.21719 u_1^2 - 4.30983 u_2 - \\ & 0.0129064 f_1 u_2 - 0.167955 f_2 u_2 - 0.861967 u_1 u_2 + 0.306487 u_2^2 \end{aligned} \tag{12}$$

for which the Hessian matrix $\mathbf{H} = 2\mathbf{A}$ is given by:

$$\mathbf{H} = \begin{pmatrix} 2.43439 & -0.861967 \\ -0.861967 & 0.612974 \end{pmatrix} \tag{13}$$

It is noted that this matrix is symmetric and positive definite because $h_{11} = 2.4349 > 0$ and $\det \mathbf{H} = 0.749228 > 0$. Therefore, the critical points u_1 and u_2, of F are the minimum points. To determine these critical points, solve the system:

$$\begin{cases} \dfrac{\partial F}{\partial u_1} = 0 \\ \dfrac{\partial F}{\partial u_2} = 0 \end{cases} \tag{14}$$

with the unknowns u_1 and u_2, obtaining:

$$\begin{aligned} u_1 &= -0.0208281 + 0.00694186 f_1 + 0.143625 f_2 \\ u_2 &= 7.00174 + 0.0308171 f_1 + 0.475967 f_2 \end{aligned} \tag{15}$$

These dependencies are shown in Figures 11 and 12.

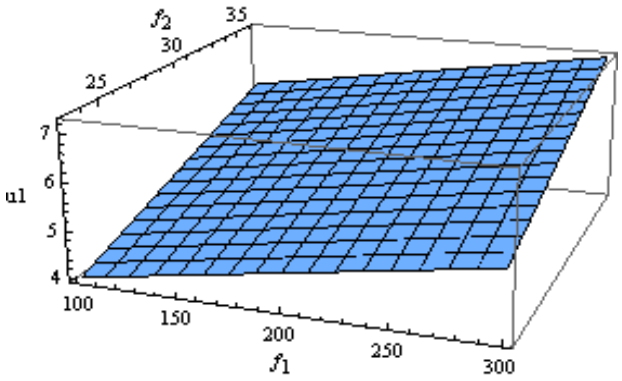

Figure 11. Dependence of u_1 on f_1 and f_2.

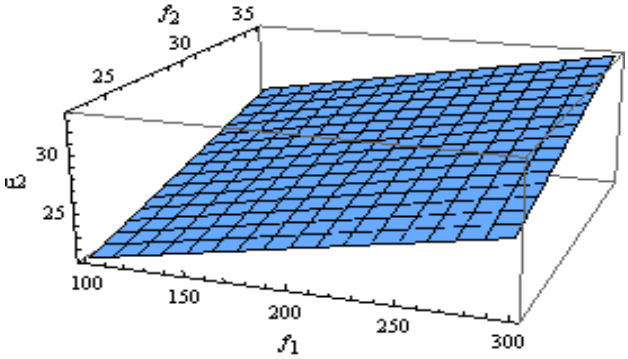

Figure 12. Dependence of u_2 on f_1 and f_2.

By substituting the values of the controlled variables u_1 and u_2 given by (15) in Eq. (12), the function F becomes:

$$\begin{aligned} F = {} & 15.2783 + 0.0000460282 f_1^2 - 0.0422479 f_1 + \\ & 0.00130056 f_1 f_2 - 0.8741 f_2 + 0.0128082 f_2^2 \end{aligned} \tag{16}$$

and represents the minimum energy consumption, depending only on the uncontrolled parameters.

The graphical representation of F is illustrated in Figure 13.

Knowing the uncontrolled variables f_1 and f_2, the values of the controlled variables u_1 and u_2 are computed by applying the proposed model and are compared to the measured values listed in Table 10.

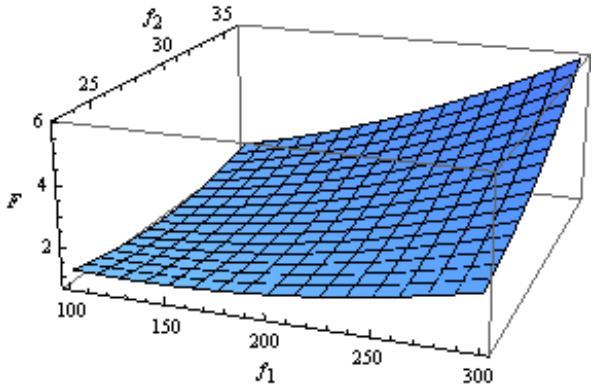

Figure 13. Simulated electricity consumption depending on f_1 and f_2.

Table 10. Comparison of computed and measured values u_1, u_2 and F

f_1 [W/m^2]	f_2 [°C]	u_1[°C]			u_2 [°C]			F [kWh]		
		Computed	Measured	Percentage difference [%]	Computed	Measured	Percentage difference [%]	Computed	Measured	Percentage difference [%]
145.20	28.6	5.09	5	1.77	25.09	25.00	0.36	0.99	1.00	–1.00
135.31	28.46	5.01	5	0.20	24.72	25.02	–1.19	0.91	0.94	–3.19
125.64	28.98	5.01	5	0.20	24.67	25.00	–1.32	0.86	0.90	–4.44
125.85	29.95	5.15	5	2.91	25.14	24.99	0.60	0.90	0.91	–1.09
122.82	30.47	5.21	5	4.03	25.29	25.05	0.95	0.91	0.96	–5.20
119.78	30.76	5.23	5	4.40	25.33	25.05	1.11	0.90	0.92	–2.17
115.04	30.97	5.23	5	4.40	25.29	25.00	1.16	0.87	0.91	–4.39

Comparing the results of the calculation with the measured values, only a small difference of 0.20-5.20% is found. Thus, optimisation of the model is validated experimentally.

The proposed model can be used in practice by implementing it in programmable electronic controllers. A simple alternative is to introduce functions that define the controlled variables u_1 and u_2, which depend on uncontrolled variables f_1 and f_2. The controller sensors measure the values of f_1 and f_2 prior to using the introduced functions to calculate u_1 and u_2, resulting in optimal control.

7. ASSESSMENT OF THERMAL COMFORT

The experimental office with the geometrical dimensions presented in Figure 2 is considered. The following data are known: indoor air temperature, 25°C; relative humidity, 43%; air velocity, 0.25 m/s; total cooling power, 3270 W; temperatures of walls with FCUs: 23.1°C, 25.1°C, 24.5°C for the systems AHU and FCUs, AHU and HRU and FCUs, respectively.

The assessment of thermal comfort in the office room is made using the PMV–PPD model [33]. A comparative study of PMV and PPD indices is performed using the computer program Thermal Comfort [34] in several points situated on a straight line (discontinuous) at different distances from the window as a function of metabolic rate (i_M) and clothing thermal resistance (R_{cl}).

Table 11. Results provided by ASHRAE Thermal Comfort program

VAC System	Distance from window [m]	1.20 met –0.60 clo			1 met – 1.01 clo			1.1 met – 0.90 clo		
		t_{mr} [°C]	PMV [–]	PPD [%]	t_{mr} [°C]	PMV [–]	PPD [%]	t_{mr} [°C]	PMV [–]	t_{mr} [°C]
0	1	2	3	4	5	6	7	8	9	10
AHU and FCUs	1.0	26.3	0.15	5	26.3	0.27	7	26.3	0.33	7
	1.5	25.9	0.11	5	25.9	0.23	6	25.9	0.28	7
	2.0	25.7	0.08	5	25.7	0.21	6	25.7	0.26	6
	2.5	25.5	0.06	5	25.5	0.19	6	25.5	0.24	6
	3.0	25.3	0.04	5	25.3	0.17	6	25.3	0.22	6
	3.5	25.2	0.03	5	25.2	0.16	6	25.2	0.21	6
	4.0	25.2	0.03	5	25.2	0.16	6	25.2	0.21	6
	4.5	25.1	0.02	5	25.1	0.15	5	25.1	0.20	6
	5.0	25.0	0.01	5	25.0	0.14	5	25.0	0.19	6
AHU	1.0	26.8	0.21	6	26.8	0.32	7	26.8	0.38	8
	1.5	26.4	0.17	6	26.4	0.28	7	26.4	0.34	7
	2.0	26.0	0.12	5	26.0	0.24	6	26.0	0.29	7
	2.5	25.8	0.10	5	25.8	0.22	6	25.8	0.27	7
	3.0	25.6	0.07	5	25.6	0.20	6	25.6	0.25	6
	3.5	25.5	0.06	5	25.5	0.19	6	25.5	0.24	6
	4.0	25.4	0.05	5	25.4	0.18	6	25.4	0.23	6
	4.5	25.3	0.04	5	25.3	0.17	6	25.3	0.22	6
	5.0	25.2	0.03	5	25.2	0.16	6	25.2	0.21	6
HRU and FCUs	1.0	27.1	0.25	6	27.1	0.35	8	27.1	0.41	9
	1.5	26.9	0.23	6	26.6	0.33	7	26.9	0.39	8
	2.0	26.7	0.20	6	26.7	0.31	7	26.7	0.37	8
	2.5	26.6	0.19	6	26.6	0.30	7	26.6	0.36	8
	3.0	26.5	0.18	6	26.5	0.29	7	26.5	0.35	7
	3.5	26.4	0.17	6	26.4	0.28	7	26.4	0.34	7
	4.0	26.3	0.15	5	26.3	0.27	7	26.3	0.33	7
	4.5	26.3	0.15	5	26.3	0.27	7	26.3	0.33	7
	5.0	23.3	0.15	5	26.3	0.27	7	26.3	0.33	7

The results of the numerical solutions obtained for the pairs of values 1.2 met–0.60 clo (standing relaxed, summer clothes), 1 met–1.01 clo (writing, normal clothes), and 1.1 met–0.90 clo (computer working, normal clothes) are reported in Table 11. In the input data

function, the mean radiant temperature t_{mr} is generated by the program. According to the performed study, it was established that the PMV index has values close to zero only for the pair of values 1.2 met–0.6 clo. For any other pair of values i_M–R_{cl}, more than 5% percent of people would be dissatisfied with their thermal comfort. In addition, in the case of AHU and FCUs system the PMV index values are lower with 28-66% and 40-93% than in the case of AHU system and HRU and FCUs system, respectively. Therefore, the first system leads to increased thermal comfort.

8. NUMERICAL SIMULATION OF ENERGY CONSUMPTION AND THERMAL COMFORT USING TRNSYS SOFTWARE

TRNSYS software [35] is one of the most flexible modelling and simulation tools and can solve complex problems from the decomposition of the model into various interconnected model components (types). One of the main advantages of TRNSYS for modelling and design is that it includes components for the calculation of building thermal loads, specific components for heating and cooling (HVAC), circulating pumps, fans, FCUs, heating and cooling coils, and chillers, as well as climatic data files, which make it a suitable tool for modelling a complete air conditioning installation to provide heating and cooling to a building.

8.1. Definition of the Operation Scheme

To simulate the electricity consumption used to cover the cooling load of the experimental room and the thermal comfort indices in the room inside, the operational connections were established between the building and all internal and external factors.

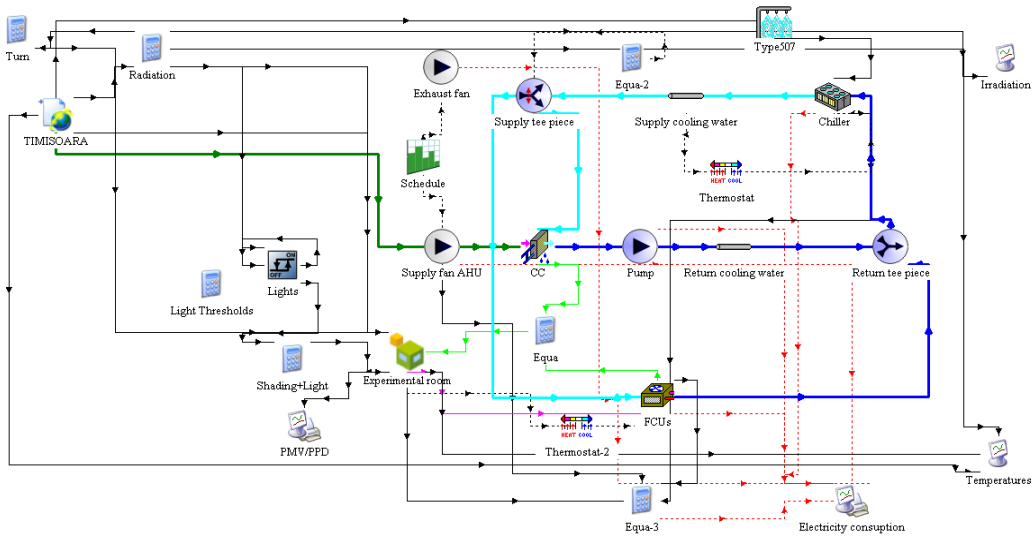

Figure 14. Scheme of the VAC system model built in TRNSYS.

Figure 14 presents the operational scheme built in TRNSYS, where the building thermal behaviour was modelled using a Type 56 subroutine. This subroutine was processed with the TRNBuild interface by introducing the main construction elements, their orientation and surface, shadow factors, and the types of indoor activity.

The simulation model took into account the interior gains, ventilation type, air exchange rate and components that can be obtained in the three configurations of the VAC system. Evaluation of PMV-PPD indices according to EN ISO 7730 is integrated in Type 56 subroutine.

8.2. Results of Electricity Consumption Simulation and Comparison to Experimental Data

The simulations were performed for 12 hours a day, from 6:00 to 18:00, resulting in the values graphically presented in Figure 15 for the outdoor air temperature t_e and cooling load Q_{cool} of the unconditioned space. The variation curve in the cooling load has a maximum at 9:00 because of the large glass surface (the owerall ratio of glass to the exterior wall is 64%) and the maximum solar radiation intensity is 695 W/m^2.

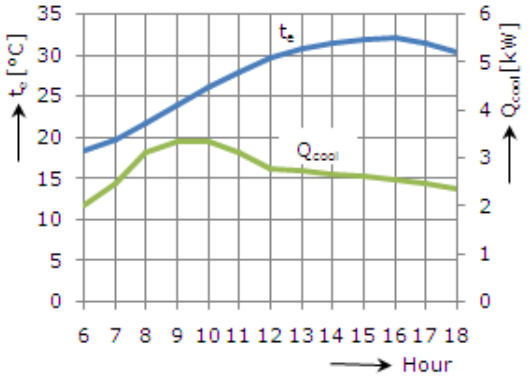

Figure 15. Simulation of the cooling load for the experimental room.

Performing simulations over a time interval of 8 working hours, the electrical energy consumption levels in the four scenarios for the AHU and FCUs system were obtained and are presented beside the measured values in Tables 12-15. For all data, the uncertainty (the difference between the TRNSYS simulated value and the measured value) of electricity consumption was less than 6.2%, 8.8%, 8.0% and 9.6% for scenarios 1, 2, 3, and 4, respectively. Thus, the simulation model was validated by the experimental data.

8.3. Simulation of Thermal Comfort Indices PMV-PPD in the Experimental Room

Using the TRNSYS program, the thermal comfort indices PMV and PPD were simulated for 12 hours a day, from 6:00 to 18:00 (Figure 16), for a set point indoor air temperature t_i of

25°C and the outdoor air temperature variation t_e shown in Figure 15. Depending on the initial data of the building, the mean radiant temperature is generated by the program. The metabolic activity of 1.2 met, the air velocity of 0.1 m/s, and the clothes thermal resistance of 0.5 clo are defined in the TRNBuild subroutine.

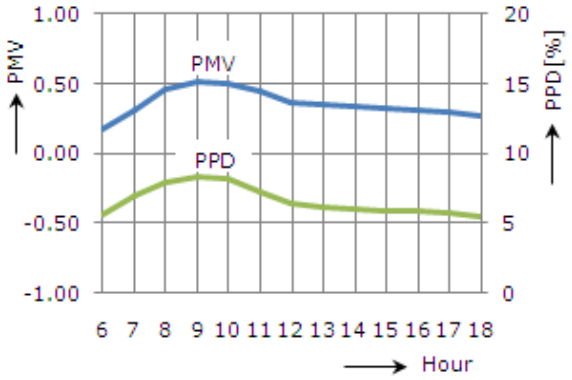

Figure 16. Simulation of the hourly variation of the PMV and PPD indices.

Table 12. Electrical energy consumption for scenario 1

Hour	Consumed energy [kWh]								Uncertainty [%]
	Simulated				Measured				
	Chiller	AHU	FCUs	Total	Chiller	AHU	FCUs	Total	
8:00	0.51	0.52	0.03	1.06	0.5	0.51	0.03	1.04	1.88
9:00	0.52	0.52	0.03	1.07	0.51	0.51	0.03	1.05	1.86
10:00	0.54	0.52	0.03	1.09	0.53	0.51	0.03	1.07	1.83
11:00	0.61	0.52	0.06	1.19	0.61	0.51	0.05	1.17	1.68
12:00	0.57	0.52	0.05	1.14	0.54	0.51	0.04	1.09	4.38
13:00	0.56	0.52	0.04	1.12	0.52	0.51	0.02	1.05	6.25
14:00	0.46	0.52	0.02	1.00	0.45	0.51	0.01	0.97	3.00
15:00	0.43	0.52	0.02	0.97	0.43	0.51	0.01	0.95	2.06
16:00	0.44	0.52	0.02	0.98	0.45	0.51	0.01	0.97	1.02

Table 13. Electrical energy consumption for scenario 2

Hour	Consumed energy [kWh]								Uncertainty [%]
	Simulated				Measured				
	Chiller	AHU	FCUs	Total	Chiller	AHU	FCUs	Total	
8:00	0.35	0.52	0.04	0.91	0.32	0.51	0.04	0.87	4.39
9:00	0.36	0.52	0.05	0.93	0.33	0.51	0.05	0.89	4.30
10:00	0.37	0.52	0.05	0.94	0.34	0.51	0.05	0.90	4.25
11:00	0.45	0.52	0.08	1.05	0.43	0.51	0.06	1.00	4.76
12:00	0.51	0.52	0.07	1.10	0.48	0.51	0.05	1.04	5.45
13:00	0.34	0.52	0.05	0.91	0.30	0.51	0.03	0.84	7.69
14:00	0.33	0.52	0.05	0.90	0.28	0.51	0.03	0.82	8.88
15:00	0.33	0.52	0.04	0.89	0.32	0.51	0.03	0.86	3.37
16:00	0.32	0.52	0.04	0.88	0.32	0.51	0.03	0.86	2.27

Table 14. Electrical energy consumption for scenario 3

Hour	Consumed energy [kWh]								Uncertainty [%]
	Simulated				Measured				
	Chiller	AHU	FCUs	Total	Chiller	AHU	FCUs	Total	
8:00	0.45	0.52	0.04	1.01	0.43	0.51	0.04	0.98	2.97
9:00	0.45	0.52	0.05	1.02	0.44	0.51	0.04	0.99	2.94
10:00	0.46	0.52	0.05	1.03	0.43	0.51	0.05	0.99	3.88
11:00	0.60	0.52	0.07	1.19	0.55	0.51	0.06	1.12	5.88
12:00	0.65	0.52	0.08	1.25	0.58	0.51	0.06	1.15	8.00
13:00	0.45	0.52	0.06	1.03	0.40	0.51	0.04	0.95	7.76
14:00	0.47	0.52	0.05	1.04	0.45	0.51	0.04	1.00	3.84
15:00	0.46	0.52	0.04	1.02	0.45	0.51	0.03	0.99	2.94
16:00	0.45	0.52	0.04	1.01	0.43	0.51	0.03	0.97	3.96

Table 15. Electrical energy consumption for scenario 4

Hour	Consumed energy [kWh]								Uncertainty [%]
	Simulated				Measured				
	Chiller	AHU	FCUs	Total	Chiller	AHU	FCUs	Total	
8:00	0.33	0.52	0.04	0.89	0.32	0.51	0.03	0.86	3.37
9:00	0.35	0.52	0.05	0.92	0.33	0.51	0.04	0.88	4.34
10:00	0.36	0.52	0.05	0.93	0.32	0.51	0.05	0.88	5.37
11:00	0.44	0.52	0.08	1.04	0.40	0.51	0.06	0.97	6.73
12:00	0.45	0.52	0.07	1.04	0.39	0.51	0.04	0.94	9.61
13:00	0.45	0.52	0.07	1.04	0.39	0.51	0.06	0.96	7.69
14:00	0.43	0.52	0.06	1.01	0.38	0.51	0.04	0.93	7.92
15:00	0.41	0.52	0.05	0.98	0.38	0.51	0.04	0.93	5.10
16:00	0.34	0.52	0.04	0.90	0.29	0.51	0.02	0.82	8.88

It is found that the PMV index has values of up to 0.5 and the PPD index ranges from 5% to 8.3%, reaching its maximum value at approximately 9:00. For the remainder of the time, the values are close to the optimal value of 5%. The results show that the conditions for thermal comfort for category B in EN ISO 7730 [26] are satisfied.

9. Influence of Indoor Design Air Parameters on EnergyConsumption of Heating and Air Conditioning

The indoor design air parameters should be determined within a range to meet both requirements of thermal comfort and building energy efficiency. This section analysed the indoor air parameters in two types of public buildings based on simulation [36].

9.1. Simulation Method

The simulation models of two types of public buildings including small office building (SO) and large office building (LO) were established by Designer's Simulation Toolkit (DeST). DeST is a tool developed for aiding the heating, ventilation and air conditioning (HVAC) engineer to conduct simulation and analysis of the performance of the HVAC system in buildings [37]. The boundary conditions of the two models were listed in Table 16.

Table 16. Model description

Characteristics	SO	LO
Building stories	5	23
Floor height	3.6 m	3.6 m
Building area	5000 m^2	40,000 m^3
HVAC system	Fan-coil system/fresh air unit	Fan coil system/fresh air unit
Heating source	Boiler	Boiler
Cooling source	Electric chiller	Electric chiller
Pump type	Single speed	Variable speed
Lighting load	14.5 W/m^2	14.5 W/m^2
People density	6 m^2/p	6 m^2/p
Facility load	16.5 W/m^2	16.5 W/m^2
Fresh air volume	30 $m^3/(h \cdot p)$	30 $m^3/(h \cdot p)$
Schedule	Daytime: 7:00-20:00 Holiday: off	Daytime: 7:00-20:00 Holiday: off
Heating period	November 15th – March 15th	November 15th – March 15th
Cooling period	June 1st – September 30th	June 1st – September 30th

PMV was used as the benchmark for the energy consumption analysis, thus $-1 \leq PMV \leq 1$ was set as the limitation for simulation models. The limitations of indoor air temperature were 16-24°C for radiator heating system (RHS) and 18-24°C for air conditioning system (ACS) in winter and 22-28°C for ACS in summer [36].

9.1.1. EnergyConsumption of Water Chillers

The small office building had one water chiller taken all the cooling loads in summer, while the large office building had two water chillers sharing cooling loads. If the partial loads were less than 50%, then only one chiller would be operated in the large office building. According to the load rate, the control mode of water chiller units can be determined. The energy consumption of water chiller for partial loads can be calculated as:

$$E_{\mathrm{WC}} = \sum P_i \tau_i \tag{17}$$

where E_{WC} is the energy consumption of water chiller, in kWh; P_i is the input power under relevant partial load rate, in kW; τ_i is the operating time for partial load, in h.

9.1.2. Energy Consumption of Heating Source

The coal consumed by the boiler during the whole heating season can be calculated as:

$$C = \frac{Q_H}{q_s \eta_{\mathrm{RHS}} \eta_b} \tag{18}$$

where C is the coal consumption, in kg; Q_H is the heat gain of the system, in J; q_s is the calorific value of equivalent (29.27 J/kg); η_{RHS} is the network transmission efficiency of RHS, which was set as 94%; η_b is the operating efficiency of boilers, which was set as 90%.

In order to uniform the unit of energy consumption, 0.404 kg coal equivalent for 1 kWh electricity was set as the conversion factor:

$$E = \frac{C}{0.404} \tag{19}$$

where E is the energy consumption of heating source, in kWh.

9.1.3. Energy Consumption of Water Pumps

The small office building had one water pump with a constant flow rate, while the large office building had two water pumps sharing constant flow rate in winter and variable flow rate in summer. If the partial loads were less than 50% then only one pump would be operated in the large office building. The energy consumption of water pump can be calculated using the equation:

$$P_p = \frac{G_p H}{\eta_p} \tag{20}$$

where P_p is the power of water pumps, in kW; G_p is the water flow rate, in m^3/s; H is the practical pressure, in kPa; η_p is the efficiencies of water pumps.

9.1.4. Energy Consumption of Fans

Fans in fresh air units and exhaust fans were taken into account in the energy consumption calculation for office buildings. The energy consumption of fans can be calculated using the equation:

$$P_f = \frac{G_f p}{\eta_f} \tag{21}$$

where P_f is the power fans, in kW; G_f is the air flow rate, in m^3/s; p is the practical pressure, in kPa; η_f is the efficiencies of fans.

9.1.5. Energy Consumption of Humidifiers

The high-voltage spayer had the working mode of iso-thermal and a minimum power of 35 W/unit. Because this type of humidifier had low requirement of water quality and low cost, it was used in the simulation models.

9.2. Simulation Results and Discussion

On the base range of 30% ≤ RH ≤ 70% and −1 ≤ PMV ≤ 1 for summer and 20% ≤ RH ≤ 60% and −1 ≤ PMV ≤ 1 for winter, the influence of indoor design air parameters on energy consumption of HVAC system were discussed [36].

It can be seen from Figures 17 and 18, the energy consumption of SO with fan-coil unit was 15-27 kWh/(m^2·a) in summer and 13-28 kWh/(m^2·a) in winter, while that of LO with fan-coil unit was 12-24.5 kWh/(m^2·a) in summer and 9.8-26.5 kWh/(m^2·a) in winter.

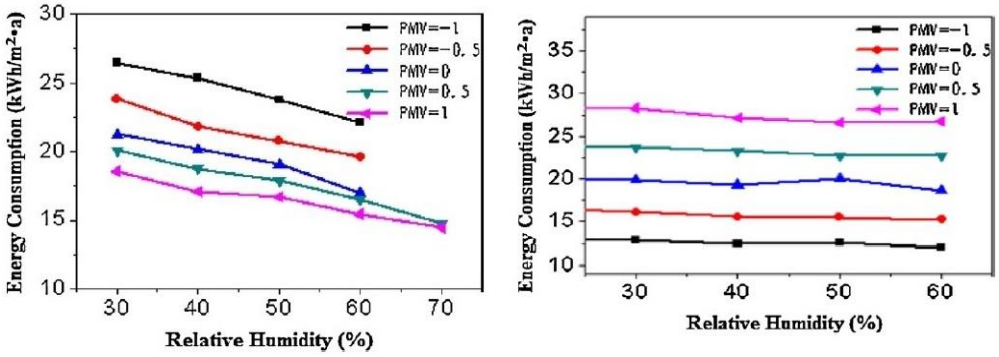

Figure 17. Energy consumption of SO in summer and winter.

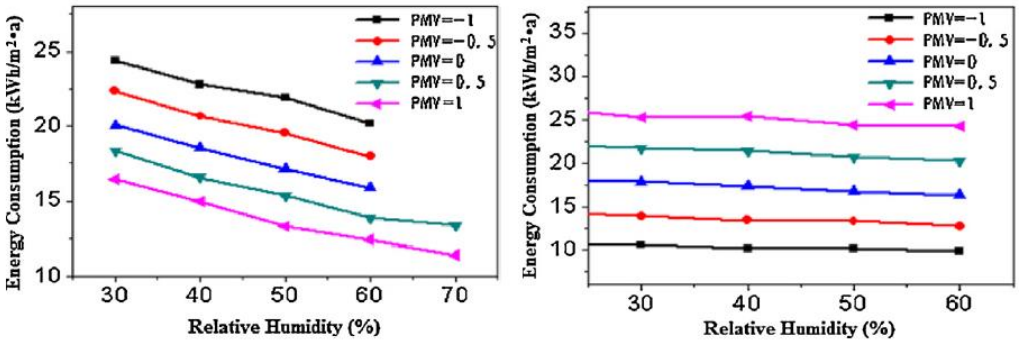

Figure 18. Energy consumption of LO in summer and winter.

Under the same level of PMV, the energy consumption would increase 5.5-6.7% for SO and 5.7-7.5% for LO with each 10% decrease of the relative humidity in summer. If the relative humidity was on the same level, the energy consumption in summer would increase 10-12% for SO and 8.1-9.7% for LO with each 0.5 decrease of PMV, while the energy consumption in winter would increase 13% for SO and 13.5% for LO with each 0.5 increase of PMV.

When the relative humidity was on the same level of 50%, variations of the energy consumption of two types of buildings under different PMV values were shown in Figures 19 and 20.

Indoor design air parameters of small office buildings had great influence on the energy consumption of fan-coil units in summer and that of heat source in winter. The energy

consumption of fan-coil unit would increase 12% with each 0.5 decrease of PMV, while that of heat source would increase 14.8% with each 0.5 increase of PMV.

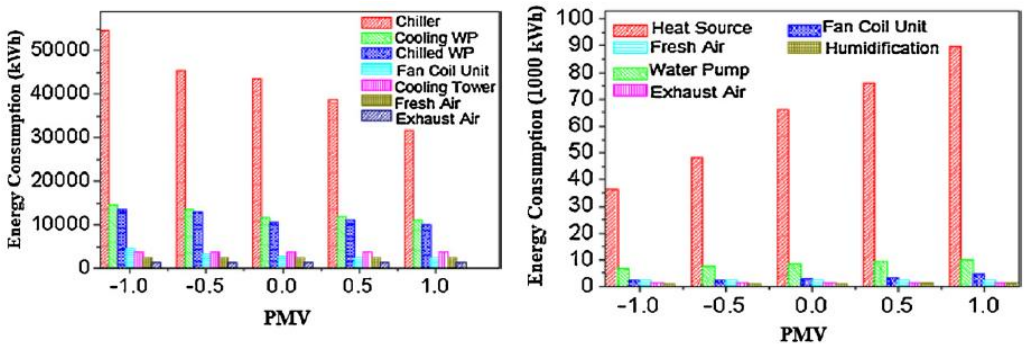

Figure 19. Energy consumption percentage of SO in summer and winter.

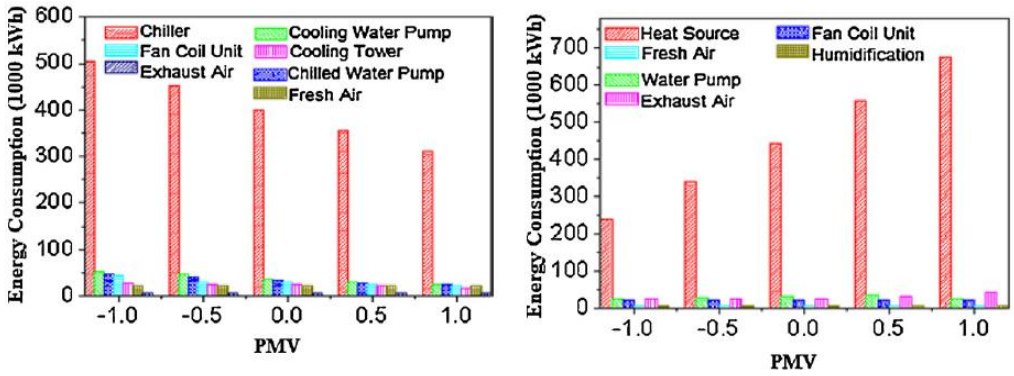

Figure 20. Energy consumption percentage of LO in summer and winter.

Indoor design air parameters of large office buildings had grat influence on the energy consumption of water pumps in summer and that of heat source in winter. The energy consumption of water pumps would decrease 12.3% with each 0.5 increase of PMV because of the variable flow rate operation mode, while that of heat source would increase 16.1% with each 0.5 increase of PMV. Besides, although the energy consumption of chillers accounted for the largest proportion in LO, the influence of different PMV values exerted more influence on the energy consumption of water pumps in summer. That is because of the variable speed control mode of the water pumps. The energy consumption of the pumps would be reduced significantly with the decrease of the water flow rate.

As for the RHS mode, the influence of indoor design air temperature varied between 17 and 27°C on heating energy consumption for office buildings. The heating energy consumption of SO was approximately 13-30 kWh/(m^2·a), while that of LO was approximately 10-23 kWh/(m^2·a). The heating energy consumption would increase 6.9-9.8% for SO and 6.5-9.7 for LO with each 1°C rise of indoor design air temperature.

From above analysis, energy efficient office buildings with fan-coil system should have relatively high relative humidity with the same thermal comfort level and relatively high PMV value with the same relative humidity in summer, while they should have a relatively

low PMV value with the same relative humidity in winter. With comprehensive consideration of indoor thermal comfort and building energy consumption, recommend ranges of indoor design air parameters for two types of buildings were summarised in Table 17.

Table 17. Recommend ranges for two types of buildings

Building type	Season	Mode	PMV [–]	PPD [%]	t_i [°C]	RH [%]
SO	Summer	ACS	0.5 < PMV < 1	≤26.1	26.2-28.2	50-70
LO	Winter	ACS	–1 < PMV < 0	≤26.1	18.0-20.7	50-70
	Winter	RHS	PMV < 0	≤26.1	17.0-22.6	

CONCLUSION

The aim of this study has been to define the VAC system configuration for office buildings with the lowest energy consumption without compromising indoor comfort. This clearly indicates that the VAC system of a building has a large potential for saving energy. A cost-effective way to improve the energy performance of a VAC system is to improve the components' efficiency and implement efficient control. Some main conclusions can be deduced from this study:

(1) To improve the chiller efficiency, a water mist system was coupled to the air-cooled condenser. The experimental results revealed that with an evaporative pre-cooling system, the power consumption decreased and the cooling capacity and EER increased considerably. The application of an evaporative pre-cooler improved the EER of an air-cooled chiller by 24.8-30.8% and it's ESEER by 13.0-13.7% under the climatic conditions of Romania.
(2) Thus, it is possible to obtain an energy saving of 1.15 to 12.96% for an AHU and FCUs system, 7.78-30.47% for an AHU system, and 4.50-39.79% for an HRU and FCUs system, depending on the chiller cooling mode and the cooled water temperature.
(3) By application of water mist pre-cooling to the air-cooled chiller, the COP_{syst} increased between 2.24 to 39.79%, depending on the VAC system. By increasing the cooled water temperature from 5°C to 8°C, the COP_{syst} increased between 1.8 and 10.7%. This demonstrates that improvements in the chiller EER have a greater influence on COP_{syst} than increasing the temperature of the cooled water.
(4) The AHU and FCUs system has a maximum energy performance (COP_{syst} = 2.24) greater than that of the AHU system (COP_{syst} = 1.60) under the conditions described previously.
(5) The HRU and FCUs system has a COP_{syst} equal to 7.12, but this system is especially recommended for residential buildings.
(6) Having the values of solar radiation intensity f_1, and outdoor air temperature f_2,the optimal values for the cooled water temperature u_1 and the indoor air temperature $u_2$can be determined and the minimum energy consumption of the system can be

obtained by the proposed mathematical model. This model can be applied in practice by implementing PLCs that use its functions to define the controlled variables u_1 and u_2 depending on the uncontrolled variables f_1 and f_2.

(7) For a given cooling load, it is found that the PMV thermal comfort index using the AHU and FCUs system is lower than that of the other two systems. Thus, in an experimental room, the PMV index of the AHU and FCUs system has 26 to 28% lower values than the AHU system and 40 to 93% lower values than the HRU and FCUs system. Therefore, the first system leads to increased thermal comfort.

(8) Comparing measured data to the results of simulations in TRNSYS for the electricity consumption in the AHU and FCUs system in four analysis scenarios, the maximum identified difference is 9.6%. Thus, the simulation model is validated. Additionally, simulating the comfort indices in an office room during a 12 hour period, the PMV value varies between 0.2 and 0.5 and the PPD index has values in the range of 5-8.3%, which corresponds to category B in EN ISO 7730 [26].

(9) The developed TRNSYS simulation model can be used as a tool to determine the AHU and FCUs system performance in different operation modes to optimise the system energy efficiency and ensure the user's comfort throughout the year.

(10) The simulation results revealed that design relative humidity in winter not only exerts negligible influence on indoor thermal comfort but also has little effect on the energy consumption.

(11) With fully considering the thermal comfort and building energy efficiency, the low bound that PMV > 0 was recommended in summer and the up bound that PMV < 0 was recommended in winter.

REFERENCES

[1] Sundell J. On the history of indoor air quality and health. *Indoor Air* 2004;14:51-58.

[2] Perez-Lombard L, Ortiz J, Pout C. A review on buildings energy consumption information. *Energy and* Buildings 2008;40(3):394-398.

[3] Sherman MH, Matson N. Residential ventilation and energy characteristics. *ASHRAE Journal* 1997;103(Pt.I):717-730.

[4] Liddament MW, Orme M. Energy and ventilation. *Applied Thermal Engineering* 1988;18(11):1101-1109.

[5] Perez-Lombard L, Ortiz J, Maestre IR. The map of energy flow in HVAC systems. *Applied Energy* 2011;88(12):5020-5031.

[6] Kolokotroni M, Aronis A. Cooling-energy reduction in air-conditioned offices by using night ventilation. *Applied Energy* 1999;63(4):241-253.

[7] Budaiwi IM, Al-Homoud MS. Effect of ventilation strategies on air contaminant concentrations and energy consumption in buildings. *International Journal of Energy Research* 2001;25(12):1073-1089.

[8] Sherman MH, Walker IS. Meeting residential ventilation standard through dynamic control of ventilation systems. *Energy and Buildings* 2011;43(8):1904-1912.

[9] Roulet CA, Heidt FD, Foradini F, Pibiri MC. real heat recovery with air handling units. *Energy and Buildings* 2001;33(5):495-502.

[10] Dodoo A, Gustavsson L, Sathre R. Primary energy implications of ventilation heat recovery in residential buildings. *Energy and Buildings* 2011;43(7):1566-1572.
[11] Nabinger S, Persily A. Impacts of airtightening retrofits on ventilation rates and energy consumption in a manufactured home. *Energy and Buildings* 2011;43(11):3059-3067.
[12] Lin Z, Lee CK, Fong KF, Chow TT. Comparison of annual energy performances with different ventilation methods for temperature and humidity control. *Energy and Buildings* 2011;43(12):3599-3608.
[13] Djongyang N, Tchinda R, Njoneo D. Thermal comfort: a review paper. *Renewable and Sustainable Energy Reviews* 2010;14:2626-2640.
[14] Sourbron M, Helsen L. Evaluation of adaptive thermal comfort models in moderate climates and their impact on energy use in office buildings. *Energy and Buildings* 2011;43:423-432.
[15] Engdahl F, Johansson D. Optimal supply air temperature with respect to energy use in a variable air volume system. *Energy and Buildings* 2004;36:205-218.
[16] Yu FW, Chan KT. Tune up of the set point of condensing temperature for more energy efficient air cooled chillers. *Energy Conversion and Management* 2006;47:2499-2514.
[17] Manske KA, Reindl DT, Klein SA. Evaporative condenser control in industrial refrigeration systems. *International Journal of Refrigeration* 2001;24:676-691.
[18] Pistochini T, Modera M. Water-use efficiency for alternative cooling technologies in arid climates. *Energy and Buildings* 2011;43:631-638.
[19] Zhang H, You H, Yang HX, Niu JL. Enhanced performance of air-cooled chillers using evaporative cooling. *Building Services Engineering Research Technology* 2000;21:213-217.
[20] Yu FW, Chan FW. Application of direct evaporative coolers for improving the energy efficiency of air-cooled chillers. *Journal of Solar Energy Engineering* 2005;127:430-433.
[21] Hajidavallo E. Application of evaporative cooling on the condenser of window-air-conditioner. *Applied Thermal Engineering* 2007;27:1937-1943.
[22] Aprea C, Renno C. An experimental analysis of a thermodynamic model of a vapour compression refrigeration plant on varying the compressor speed. *International Journal of Energy Research* 2004;28:537-549.
[23] Koury RN, Machado L, Ismail KA. Numerical simulation of a variable speed refrigeration system. *International Journal of Refrigeration* 2001;24:192-200.
[24] EN 15251, Indoor Environmental Input Parameters for Design and Assessment of Energy Performance of Buildings Addressing Indoor Air Quality, Thermal Environment, Lighting and Acoustics, European Committee for Standardization (CEN), Brussels, 2007.
[25] Sarbu I, Adam M. Experimental and numerical investigations of the energy efficiency of conventional air conditioning systems in cooling mode and comfort assurance in office buildings. *Energy and Buildings* 2014;85:45-58.
[26] GesslerW, Müller S, Neuhuber J, Radk R. Chillers planning manual. Herne, Germany: GEA Klimatechnik GmbH and Co KG; 2008.
[27] http://solar.physics.uvt.ro/srms/.
[28] Holman JP. Experimental method for engineers, Singapore: McGraw Hill; 2001.
[29] Sud I. Control strategies for minimum energy usage. *ASHRAE Transactions* 1984;90(2):247-277.

[30] Lau AS, Beckman WA, Mitchell JW. Development of computer control routines for a large chilled water plant. *ASHRAE Transactions* 1985;91(1):780.
[31] Braun JE. Methodologies for design and control of central cooling plants. Doctoral thesis, Department of Mechanical Engineering, University of Wisconsin-Madison, USA; 1988.
[32] Ulleberg O. Emulation and control of heating, ventilation, and air-conditioning systems. Master of Science Thesis, University of Wisconsin-Madison, USA; 1993.
[33] Sarbu I, Sebarchievici C. Aspects of indoor environmental quality assessment in buildings. *Energy and Buildings* 2013;60:410-419.
[34] ASHRAE Thermal comfort tool, Version 2. Berkeley, California, USA: Centre for the Built Environment; 2011.
[35] TRNSYS 17 Manual, Multizone building modeling with Type 56 and TRNBuild. USA: Solar Energy Laboratory, University of Wisconsin-Madison; 2012.
[36] Ding Y, Fu Q, Tian Z, Li M, Zhu N. Influence of indoor design air parameters on energy consumption of heating and air conditioning. *Energy and Buildings* 2013;56:78-84.
[37] Manuals for DeST-C. DeST group of Tsinghua University. http://dest.tsinghua.edu.cn.